



In vitro Antibacterial Activity of Maleamates Functionalized-Chitosan-PVC/Silver Nanocomposites



Reham A. Abdel-Monem, Samir T. Gaballah, Hosam A. El-Nazer, Samira T. Rabie*

Photochemistry Department, National Research Centre, El Buhouth St., Dokki 12622, Giza, Egypt

POLY(vinyl chloride), PVC, was aminated via reaction with ethylenediamine before conjugation with functionalized chitosan (Cs) using chloroacetyl chloride as a linking agent. Cs was functionalized with p-nitrophenyl (MA), p-anisyl (MB), and p-toluy (MC) maleamates. Functionalized Cs-PVC conjugation was effected in the presence of AgNO₃ (3% w/w) producing MA-CCs-PVC/Ag nanocomposites via a one-pot synthesis method. The chemical structures of the synthesized samples were studied by FTIR spectroscopy. Scanning and transmission electron microscopy were performed to investigate the morphology of the nanocomposites, while the EDX spectrum determined Ag contents in the prepared samples. Values of water uptake measurements determined the swelling properties of the prepared nanocomposites. The antibacterial efficiency of the modified polymers was investigated against two Gram-positive (*Bacillus subtilis* and *Staphylococcus aureus*), and two Gram-negative (*Escherichia coli* and *Pseudomonas aeruginosa*) bacteria, in comparison with that of Cs, amino-PVC (Am-PVC), and ampicillin as a reference antibacterial agent.

Keywords: Chitosan, Amino-PVC, Silver nanoparticles, Antibacterial evaluation

Introduction

Infection with microorganisms is remaining one of the most serious problems in several areas of medical application. The most important medical devices that have been used on a large scale of applications are equipment for dental surgery, hospital and health care facilities, and hygienic applications [1]. Medical device polymers are considered to be important precursors in fighting off many infectious microorganisms and they have direct effects on patient's health [2-4]. When these medical polymers are implanted inside human bodies, they may become suitable places for bacterial adhesion, breeding, that can be finally followed by microbial infections, and this is considered to be one of the serious clinical complications [5]. Synthesis of antimicrobial polymers has now great importance and represents a great challenge due to its huge

applications in various medical fields. So, the interest of the development of medical polymers with anti-infective properties is largely increased to enhance their applications in the biomedical industry. To obtain these medical polymers that have high anti-infective properties, they can be compounded with some antimicrobial agents [6]. Medical devices or prostheses must be fabricated from biomaterials [7], if they are designed for implanting in the living body for a long time.

Synthetic polymers form the most diverse class of biomaterials and polyvinyl chloride (PVC) is among these polymers, as it is applied on a large scale for medical applications. PVC has been widely used for manufacturing of indwelling catheters and many hospital care medical devices [8]. Enhancing the antibacterial properties of PVC can be attained via its surface modification using an antibacterial agent as zirconium phosphate

*Corresponding author e-mail: str_strabie@yahoo.com, Tel. 01022455057

Received 17/07/2019; Accepted 27/08/2019

DOI: 10.21608/ejchem.2019.14908.1904

©2020 National Information and Documentation Center (NIDOC)

containing silver. Oxygen-plasma and azidation treatment, as well as antibiotic impregnation into the polymer matrix have been examined in recent years [9-10]. PVC wastes are, unfortunately considered to be one of the most environmental impacts that need suitable solutions for both environmental basis and economic reasons. To achieve this goal, PVC could be converted into an eco-friendly substrate by adding some nontoxic biodegradable materials [11]. It is of great interest to obtain hybrids of natural polymers with synthetic polymers as biodegradable and biomedical materials to be utilized in various applications.

Chitosan (Cs), as a natural polymer, has attracted much attention due to its excellent biological properties. Cs like many other Polysaccharides [12] is characterized by good biodegradability in the human body, antibacterial, and wound-healing activities [13-14]. Chemical modifications of PVC as an important applicable synthetic polymer with Cs as a natural biodegradable polymer can be attained via compounding Cs into PVC matrix and this may lead to the formation of a bio composite with high biodegradable and antimicrobial properties [15]. It is well known also that the solubility of Cs can be only attained in limited types of dilute acidic solutions. So, chemical modifications of Cs became of great interest in order to enhance its solubility properties with maximizing its fields of applications [16-17]. Cs is characterized by many desired properties as antimicrobial activity, the ability of bio-film-formation, and its capability to interact with various substances [18]. Subsequently, these characteristics enhance Cs to be employed in different fields of medical and pharmaceutical applications; in particular for drug release [19], continuing in the development of orthopedic devices. Cs and its derivatives can also be used to avoid tissue adhesions in post-surgical [20-21]. It is considered that nanoparticles are of a viable alternative to antibiotics. These nanoparticles seem to have a potency to overcome the problem of bacterial multidrug resistance [22]. Among these nanoparticles is silver which is well known, since ancient times, by its anti-bacterial effects and the ability to prevent and control of disparate infections [23]. It is also found that silver (AgNPs) nanoparticles have been used as an antiseptic and antimicrobial agent against Gram-positive and Gram-negative bacteria [24-25] with low cytotoxicity [26]. AgNPs were incorporated into the blended matrix of Cs-PVC

to give a new Cs-PVC/Ag as antimicrobial self-sterilizing nanocomposite that can be used in bio medicals [15,27].

Guided by the above observations, and in continuation of our previous work in this field of the synthesis of bioactive polymers [28-29], we report here a convenient synthesis of novel maleamate-functionalized Cs-PVC/AgNPs by the reaction of amino-PVC with Cs using chloroacetyl chloride as a linking agent between the Cs and PVC polymeric chains, and maleamic acid derivatives (*p*-nitrophenyl, *p*-anisyl, and *p*-toluyl) were used as Cs modifiers in presence of AgNO₃. The obtained modified nanocomposites were characterized by FTIR spectroscopy, scanning (SEM) and transmission (TEM) electron microscopy. Water uptake affinity of the three nanocomposites as well as their antibacterial activities against some of the Gram-positive and Gram-negative bacterial strains were also investigated.

Experimental

Materials

Cs (MW 100-300 kDa, 82% degree of deacetylation) was obtained from Funakoshi Co., Ltd, Japan. Suspension PVC, with a K value of 70, was obtained from A1-Ameria Company for Petrochemicals, Alexandria, Egypt. Silver nitrate was of laboratory-grade chemicals. All chemicals are of fine grades and all solvents are distilled before use. Tetrahydrofuran (THF) was distilled over potassium under N₂.

Preparation of maleamic acid derivatives

General procedure

The synthesis of maleamic acid derivatives was performed according to modification of previous work [30-33] by dissolving the corresponding amine derivatives, *p*-nitroaniline, *p*-anisidine, and *p*-toluidine (0.005 mol) in dioxane. To this solution maleic anhydride (0.49 g, 0.005 mol) dissolved in methanol (25 mL) was added drop wisely with constant stirring. The mixture was stirred at 0-5 °C for 2 h. The precipitate was filtered off and washed with diethyl ether and finally crystallized from dioxane. Three maleamate derivatives namely, *p*-nitrophenyl maleamate (M_A), *p*-anisyl maleamate (M_B), and *p*-toluyl maleamate (M_C) were obtained.

Preparation of 4-((4-nitrophenyl)amino)-4-oxobut-2-enoic acid (M_A).

M_A was obtained as described previously from *p*-nitroaniline and maleic anhydride. Color: Yellow powder; Yield: 92%; mp. 190-192°C.

Preparation of 4-((4-methoxyphenyl)amino)-4-oxobut-2-enoic acid (M_B).

M_B was obtained as described previously from *p*-anisidine and maleic anhydride. Color: Pale yellow powder; Yield 90%; mp. 191-192°C.

*Preparation of 4-oxo-4-(*p*-tolylamino)but-2-enoic acid (M_C).*

M_C was obtained as described previously from *p*-toluidine and maleic anhydride. Color: Pale yellow powder; Yield 87%; mp. 194-195°C. The chemical structure of the three maleamates (M_A, M_B, and M_C) derivatives was confirmed by FT-IR spectroscopy. FTIR (KBr, cm⁻¹): 3445 (NH); 3018 (OH, acidic); 1738 (C=O, acidic); 1642 (C=O, amidic); 1610 and 1421 (C=C, aromatic); 1639 (C=C, aliphatic).

Preparation of amino-PVC

PVC (6.2 g, 0.1 mol) was stirred in tetrahydrofuran (THF; 30 mL) overnight at room temperature to ensure complete dissolution. Ethylenediamine (3.34 mL, 0.05 mol) was added to the mixture, and then refluxed for 5 hours. Amino-PVC was collected by pouring the reaction mixture on cold MeOH/H₂O (2:1) and the reaction mixture was kept in the freezer overnight. The white solid polymer was separated by filtration followed by drying in an oven at 60°C until constant weight [34].

One-pot synthesis of maleamate-functionalized Cs-PVC/AgNPs

Swelling of both Cs (1.07g, 0.007 mol) and amino-PVC (1 g) was attained by soaking each polymer separately in dimethyl formamide (DMF) overnight. To the pre-swelled Cs was drop wisely added chloroacetyl chloride (0.55 mL, 0.007 mol) in the presence of AgNO₃ (3%, w/w, relative to Cs), with the addition of triethylamine (TEA; 3 mL) for 1 h with stirring at 0°C. The reaction mixture was left to cool and this was followed by addition of the pre-swelled amino-PVC and 10% molar ratio of each maleamate derivative (M_{A-C}) as a modifier, separately, in the presence of *N,N'*-dicyclohexyl carbodiimide (DDC; 1.36 g, 0.66 mol), as an amidation catalyst. The reaction

mixture was heated for 20 h at 55 °C, cooled, precipitated in cold MeOH/water, and filtered. The product was washed with MeOH, acetone, and ether then dried in the oven at 50 °C until constant weight to give buff solid products.

Characterization of modified maleamate-Cs-PVC/AgNPs

FTIR spectroscopy

FTIR spectra were recorded on Shimadzu IR-Spectrophotometer (FTIR 8201) Japan, at 25°C within the wavenumber range of 4000 to 400 cm⁻¹ using KBr discs.

Scanning Electronic Microscopy (SEM)

The dry samples were spread on a conducting adhesive tape, pasted on a metallic stub. The morphologies of the tested samples were investigated and imaged with a scanning electron microscope (SEM) (QUANTA FEG 250 ESEM, USA). This was accompanied by energy dispersive X-ray spectroscopy (EDAXAMETEK Inc.; Mahwah, NJ, USA) at an acceleration voltage of 15 kV. The films were fixed on the surface of sticky tape.

Transmission Electron Microscopy (TEM)

Micrographs of the colloidal particles were taken using JEOL JEM-2100(JEOL, Japan), of 200 kV with magnification range from 1000x to 50000x. The TEM samples were prepared and placed on a copper grid by mixing one dilute drop of prepared aqueous particles dispersed in 5 mL acetone to become a slightly turbid solution and allowing it to dry well. The images of representative areas were captured at suitable magnifications which clarify the morphology and the size of the nanoparticles.

Thermogravimetric Analysis (TGA)

Thermogravimetric analysis was carried out on TGA-50H thermogravimetric analyzer, Shimadzu, Japan. Samples were heated up to 600 °C in a platinum pan with a heating rate of 10 °C /min in an N₂ atmosphere of flow rate 25 mL/min.

Determination of water uptake of maleamate-functionalized Cs-PVC/AgNPs

A sample of 0.5 g of the nanocomposite was immersed in distilled water at 30 °C for 72 h, in distilled water and in buffered solutions of different pH values (4, 7, and 9). The weight of the swollen samples was determined after removal of

the surface liquid with lint-free tissue paper. The water uptake was then calculated according to the following equation.

$$W_u = [(W_f - W_o) / W_o] \times 100$$

Where W_u , W_f and W_o are water uptake, final weight, and initial weight of the sample, respectively [35]. The obtained results represent the average of three comparable experiments for each sample.

Determination of antibacterial activity

Antibacterial activity of the tested samples was evaluated using a modified Kirby-Bauer disc diffusion method [36]. Briefly, 100 mL of the tested bacteria were grown in 10 mL of fresh media until they reached a count of approximately 108 cells/mL for bacteria [37]. Microbial suspension (100 mL) were spread onto agar plates corresponding to the broth in which they were maintained. Isolated colonies of each organism, that might be playing a pathogenic role, should be selected from primary agar plates. They were examined for susceptibility by disc diffusion method [38] of the many media available, National Committee of Clinical Laboratory Standards (NCCLS) recommends Mueller-Hinton agar due to its good results in batch-to-batch reproducibility. Antibacterial activity of the prepared hydrogels was investigated against two types of Gram-positive bacteria (*B. Subtilis* and *S. aureus*), and two types of Gram-negative bacteria (*E. coli*, and *P. aeruginosa*). Plates were inoculated with bacteria at 35–37 °C for 24–48 h [36]. Standard discs of ampicillin as antibacterial agents (100 mg/mL) have served as positive controls for antibacterial activity, while (distilled water, chloroform, DMSO) have been used as a negative control. The agar used is Mueller-Hinton agar that is rigorously tested for composition and pH. Further, the depth of the agar in the plate is considered to be a factor in the disc diffusion method. This method is well documented and standard inhibition zones have been determined for susceptible and resistant values. Blank paper discs (Schleicher and Schuell, Spain) with a diameter of 8.0 mm were impregnated with 10 µl of the tested concentration of the stock solutions. When a filter paper disc, impregnated with a tested chemical is placed on agar, the chemical will diffuse from the disc into the agar. This diffusion will place the chemical on the agar only around the disc. The size of the area of the chemical infiltration around the disc was determined by the solubility of the

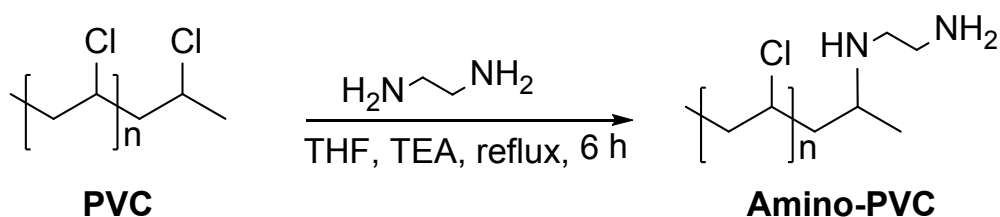
chemical and its molecular size. If an organism is placed on the agar, it will not grow around the disc if it is susceptible to the chemical. This area of no growth around the disc is known as a “zone of Inhibition”. For the disc diffusion, the zone diameters were measured with slipping calipers of the NCCLS [37]. Agar-based methods such as E-test and disc diffusion are considered to be good alternatives because they are simpler and faster than broth-based methods [39–40].

Results and Discussion

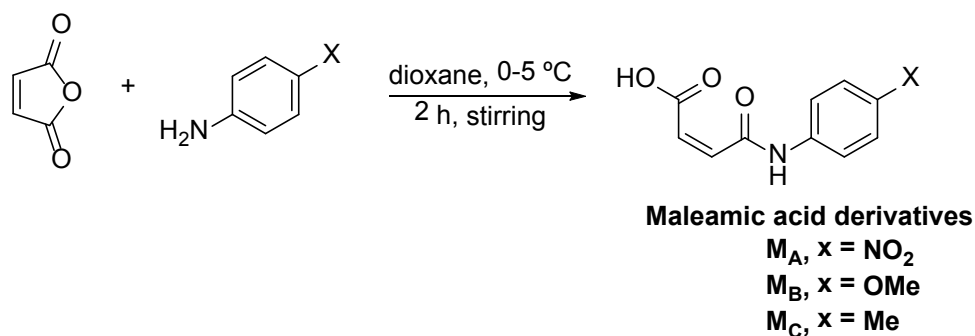
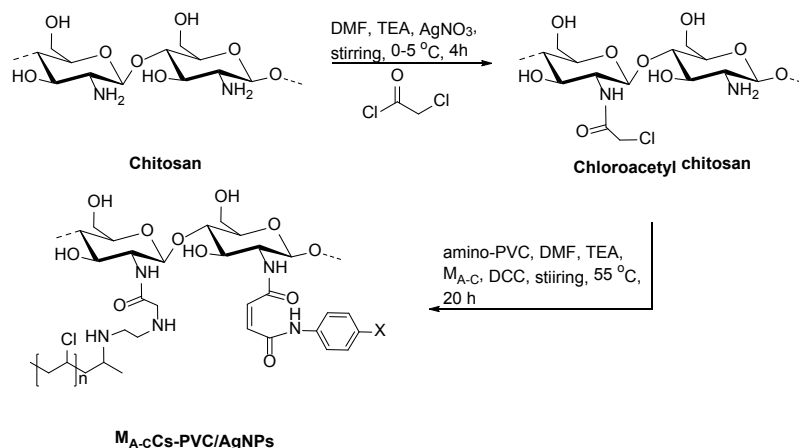
The most important requirements for PVC to be applied in various fields of biomedical are its biodegradability as well as its antibacterial activity. This was achieved previously by different techniques such as introducing the natural biodegradable polymer Cs and AgNPs as antibacterial agent [15, 27]. Therefore, this study concerns with enhancing both biodegradability and antibacterial properties of PVC to be used in biomedical applications. Modifications of both PVC and Cs were carried out to facilitate their chemical reaction. Thus, PVC was aminated using ethylenediamine which is represented in Scheme 1. The main fruitful constituents to achieve this goal are Cs and AgNPs as well as the three maleamic acid derivatives. These derivatives of maleamic acid are *p*-nitrophenyl (M_A), *p*-anisyl (M_B), and *p*-toluyl (M_C) to obtain three modified Cs-PVC polymeric conjugates with enhanced antibacterial activity (Scheme 2), whereas Cs reacted with chloroacetyl chloride to establish chloroacetyl Cs (Scheme 3). One-pot synthesis approach was performed to obtain these three M_{A-C} Cs-PVC conjugates and AgNPs were generated *in situ* by adding of $AgNO_3$ (3% *w/w*) with respect to Cs. The three synthesized nanocomposite derivatives were M_A Cs-PVC/AgNPs, M_B Cs-PVC/AgNPs, and M_C Cs-PVC/AgNPs. Incorporation of the maleamic acid derivatives as modifiers to increase the antibacterial behavior of PVC to be subjected in biomedical uses was based on many previous trials stated that such derivatives and *N*-substituted maleimides have significant antibacterial activity against some microorganisms [41–42]. Scheme 3 represents the formation of the modified maleamate-Cs/Am-PVC/AgNPs nanocomposites.

FTIR of M_{A-C} Cs-PVC/AgNPs

The chemical structures of the M_{A-C} Cs-PVC nanocomposites were studied using FTIR spectral data. The IR spectra of amino-PVC, Cs as well as M_B Cs-PVC are presented in Figure 1. The IR



Scheme 1. Synthesis of amino-PVC.

Scheme 2. Synthesis of maleamic acid derivatives (M_{A-C}).Scheme 3. One-pot synthesis of M_{A-C}Cs/PVC/AgNPs.

spectrum of amino-PVC showed a peak at 3444 cm^{-1} which is considered to be related to NH, NH_2 stretching, and the other band that was appeared at 1641 cm^{-1} was assigned to NH bend indicated the incorporation of ethylenediamine moiety with its amino groups in the backbone chains of PVC. Aliphatic (CH, and CH_2 , st.) of PVC chains are characterized by the observed IR peaks at 2979 and 2906 cm^{-1} , respectively. Two characteristic IR peaks have appeared at 1095 and 695 cm^{-1} are correlated to the (C-N) and (C-Cl), respectively. These spectral data are confirmed according to

previous work [43]. Figure 1 also showed the IR spectrum of Cs for comparison, and the observed IR peaks are in accordance with those obtained previously [44]. Both O-H and N-H stretch bands have appeared at 3444 cm^{-1} whereas these bands appeared at 2924 and 2850 cm^{-1} were correlated to C-H and CH_2 , respectively. The amide carbonyl group stretch has appeared at 1635 cm^{-1} while the two bands at 1430 and 1380 cm^{-1} were corresponding to the C-H bend. The IR bands that appeared at 1158, 1083, 1022 cm^{-1} were related to the stretch vibrations of C-O and

C-C that characterized the glucopyranose ring of Cs. The chemical structure of the OMe derivative of the modified polymers, M_B Cs-PVC, is shown and confirmed by the given IR peaks. The two IR peaks that have appeared at 1703 and 1654 cm^{-1} may be due to the amidic carbonyl stretch vibrations of the modifier maleamate moiety with its two amide C=O groups and that of Cs-linker-PVC chain respectively. In addition to these peaks, the presence of the other characteristic IR peaks of both Cs and amino-PVC confirmed that the chemical modification process of PVC with modified Cs.

Scanning electron microscopy of M_{A-C} Cs-PVC/AgNPs

The SEM images of M_{A-C} Cs-PVC/AgNPs are presented in Figure 2. AgNPs appear with good distribution along the whole matrix, in particular for samples A and B and as white spots for sample C. It is obvious that AgNPs are well immobilized by Cs functional groups [45]. SEM images show also that silver nanostructures have been synthesized and deposited without entrapping among the chains through the modified Cs matrix. AgNPs are steadily dispersed for the

modified M_{A-C} Cs-PVC nanocomposites and they are uniformly spread through these samples but to less extent in case of the *p*-toluyl maleamate derivative. This may be due to the role played by both nitro and methoxy groups that assists in the stabilization of AgNPs due to their larger sizes than the methyl group of *p*-anisyl maleamate derivative. Additionally, the electronegativity of the nitro group can be another factor that boosts the electrostatic interaction toward AgNPs. The EDX spectra of the three samples is represented in Figure 2(a-c) and determined the Ag contents in them with percentages as 3.17, 1 and 1.02 %, respectively.

Transmission electron microscopy of maleamate-Cs/Am-PVC/AgNPs

Figure 3 shows the TEM micrographs of Cs-PVC/AgNPs modified with the three maleamate derivatives. Images show transparent central areas, in particular modified samples (B) and (C), with dense dots representing the loaded silver nanoparticles into modified Cs matrix. The distributed black spots in modified Cs proved the good deposition of silver nanoparticles into the polymeric matrix. TEM images also showed that

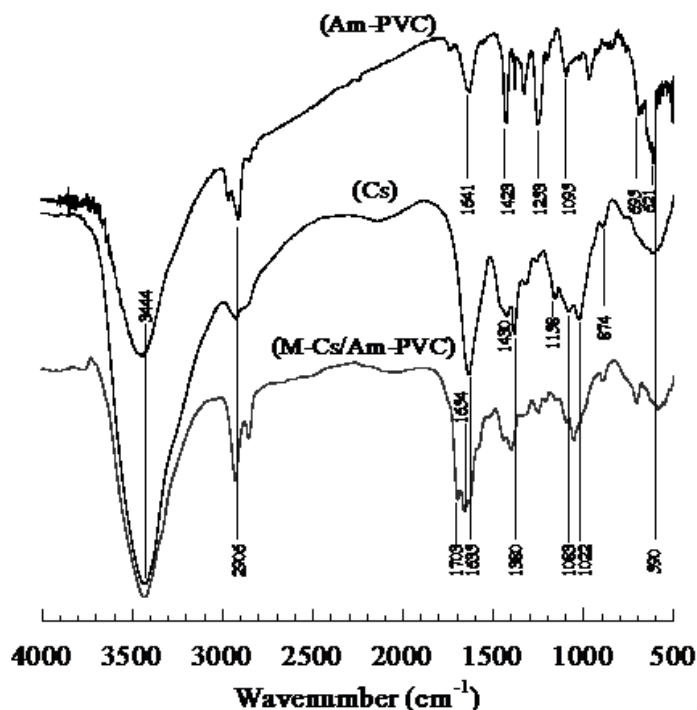


Fig. 1. FTIR spectra of Cs, amino-PVC, and MBCs-PVC.

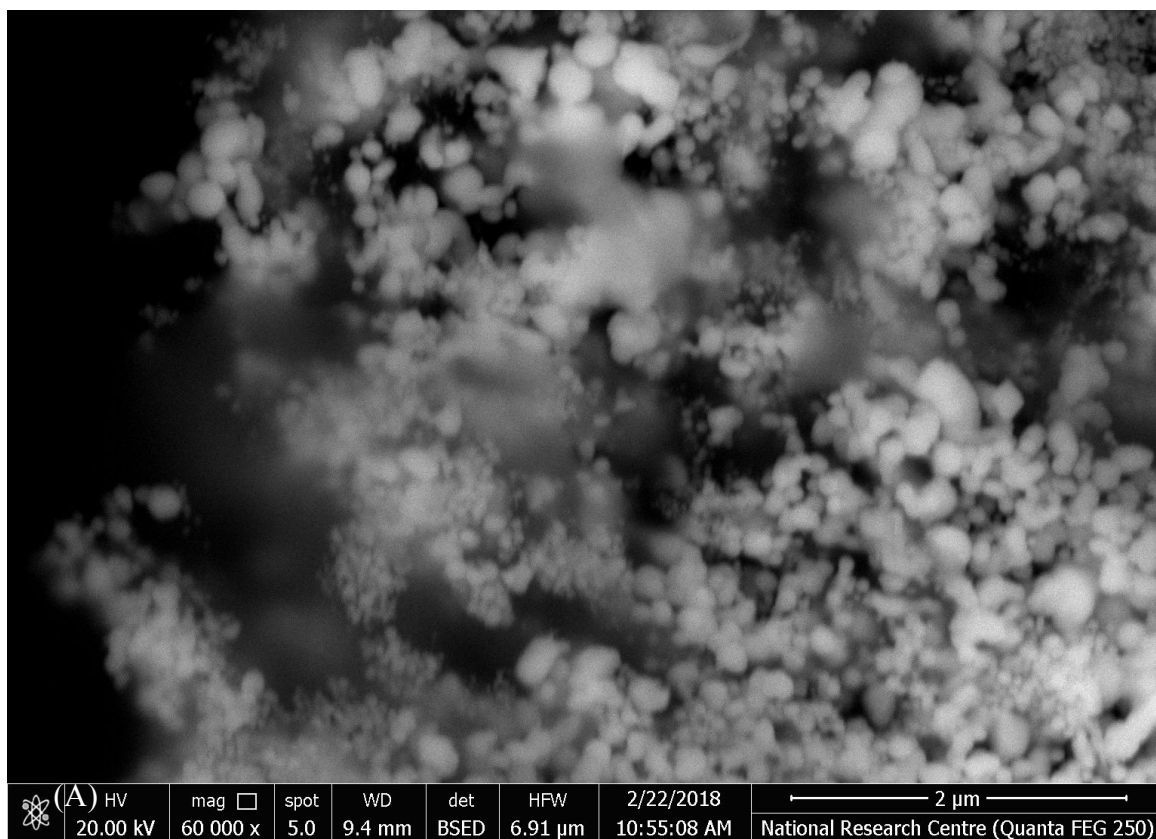


Fig. 2(A)

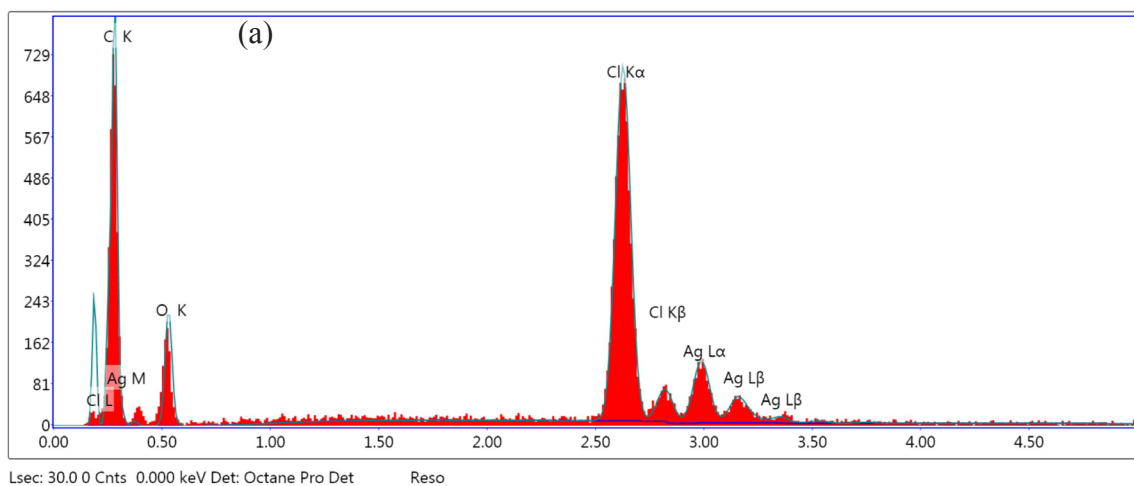


Fig. 2(a).

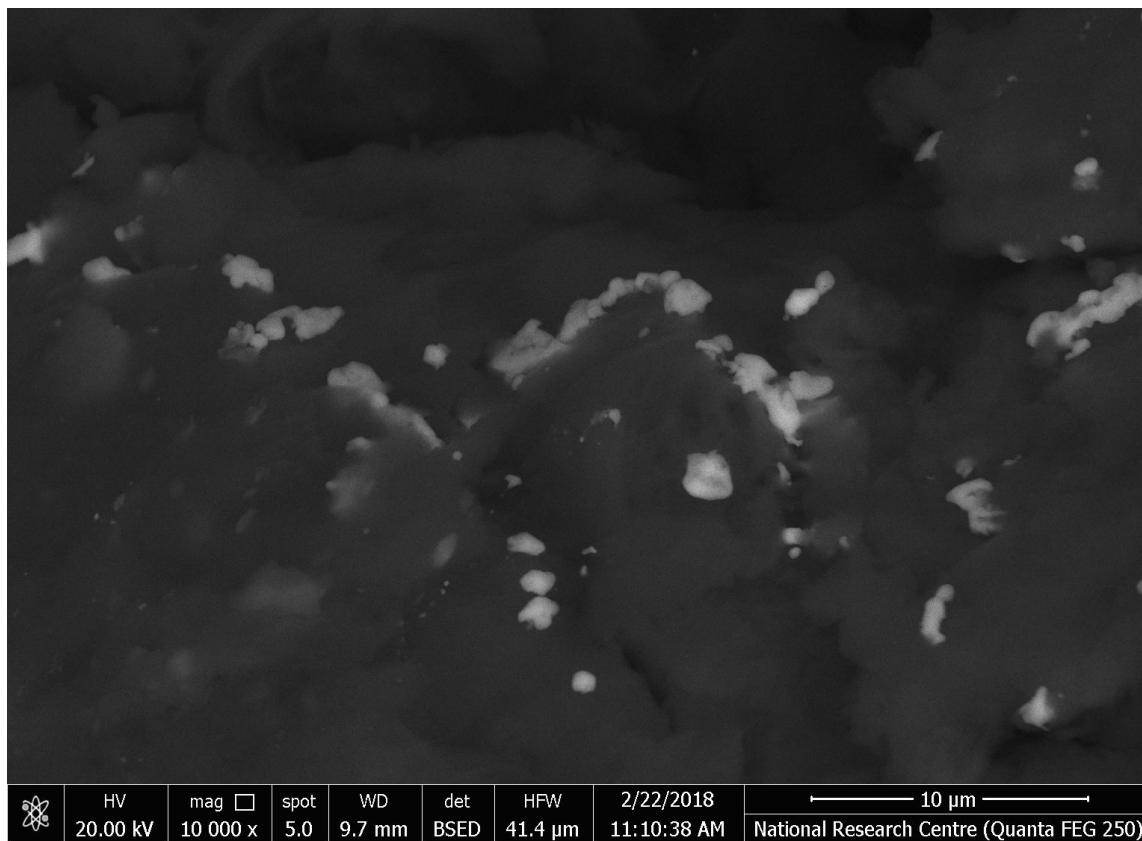


Figure 2(B).

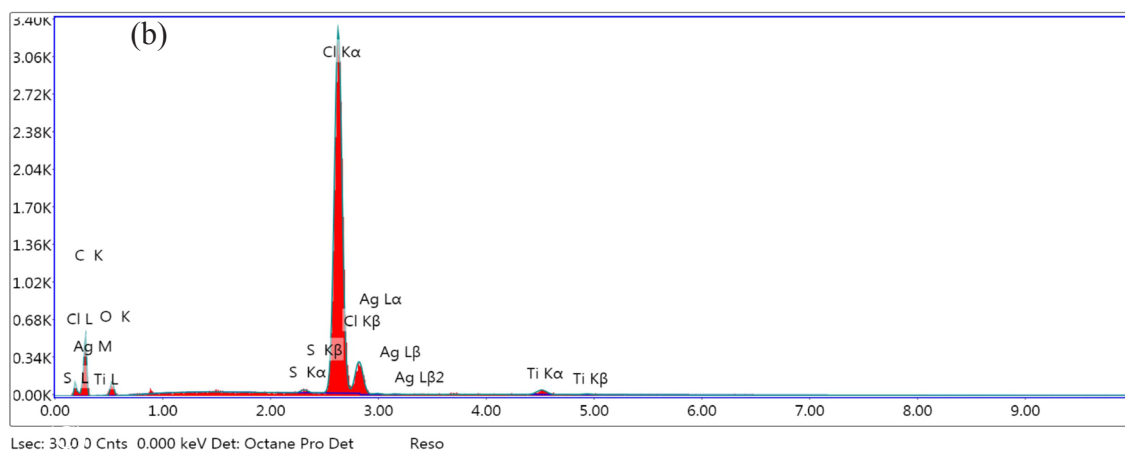


Figure 2(b).

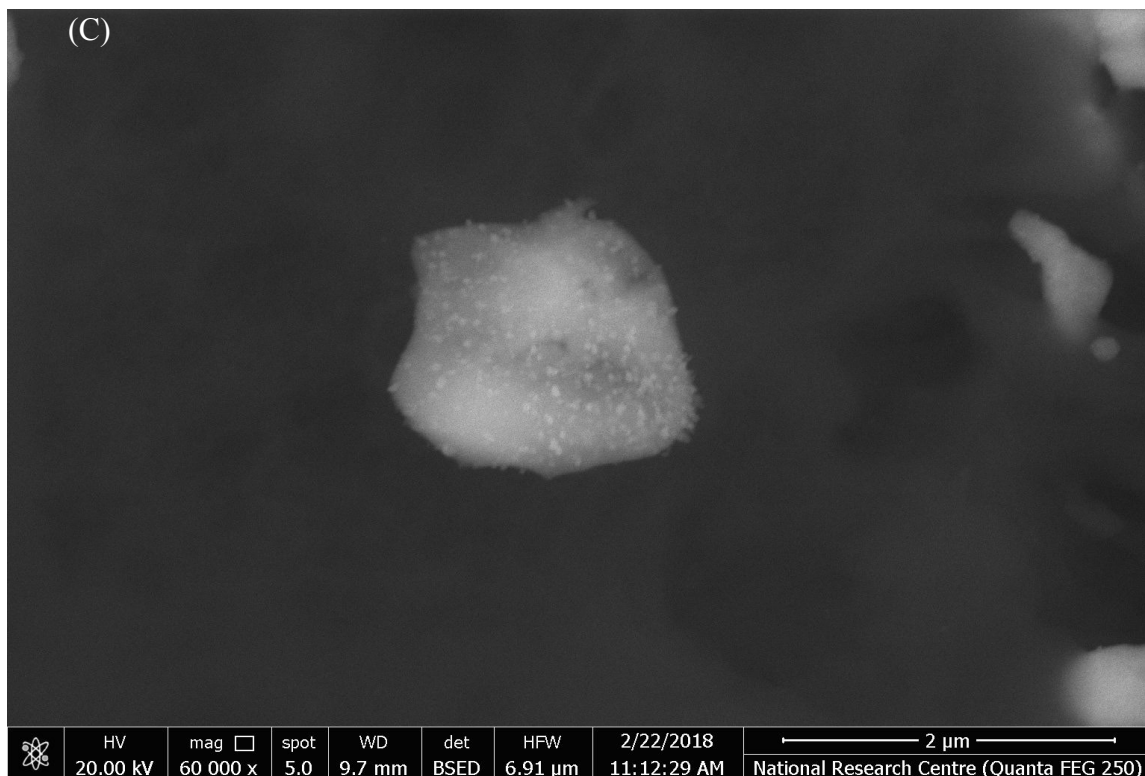


Figure 2(C).

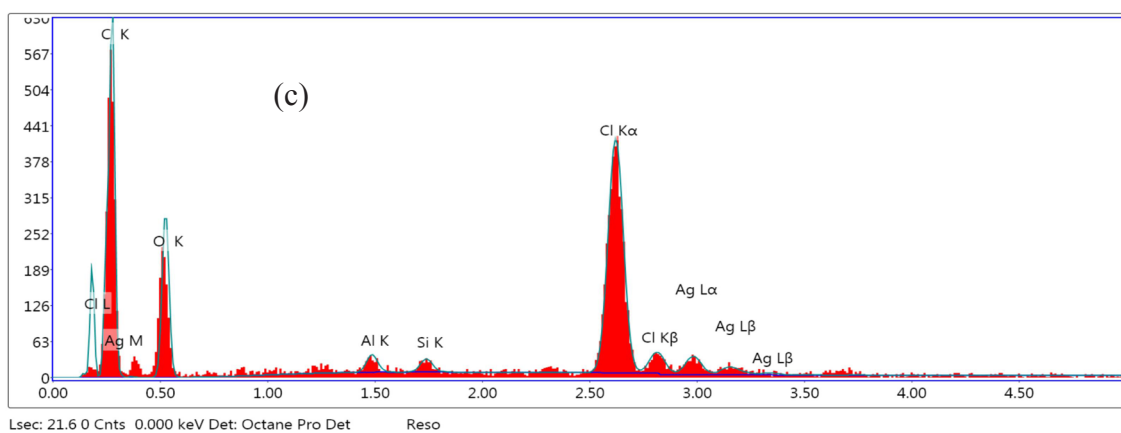


Fig. 2(c).

Fig. 2. (A) SEM micrographs for M_A Cs-PVC/AgNPs and (a) its EDX spectrum, (B) SEM micrographs for M_B Cs-PVC/AgNPs and (b) its EDX spectrum, and (C) SEM micrographs for, M_C Cs-PVC/AgNPs and (c) its EDX spectrum.

AgNPs are well embedded inside the Cs structure with formation of some aggregates. It is clear that AgNPs are distributed in a uniform manner and the average size of AgNPs is ranged between 3 and 29 nm.

Thermogravimetric Analysis of M_{A-C} Cs-PVC/AgNPs

Thermal stability of the prepared modified M_{A-C} Cs-PVC/AgNPs was investigated by thermogravimetric analysis technique, TGA. Figure 4 represents the thermal decomposition diagram of the three samples of M_{A-C} Cs-PVC/AgNPs (A, B, and C) which is compared with that of amino-PVC. The thermogram easily showed the high thermal stability of the modified polymers nanocomposite with respect to the amino -PVC one. This may be attributed to the attachment of the maleamic acid derivative moiety to the backbone chains of the polymeric substrate as well as the presence of AgNPs that enhanced the thermal stability of modified samples. As shown from Figure 4, the thermal decomposition started for the M_A Cs-PVC/AgNPs (A), M_B Cs-PVC/AgNPs (B), M_C Cs/amino-PVC/AgNPs (C), and amino-PVC at about 365 °C, 325 °C, 300 °C, and 265 °C, respectively. It is also noticed that 10% weight loss of the same samples in the same order took place at 370 °C, 345 °C, 310 °C, and 290 °C, respectively. At this stage, the weight loss may be due to loss of any residual water molecules that attached to the polymeric substrate or volatilization process of solvents present between the polymeric chains. At higher temperatures, at about 500 °C, the loss of mass of the various samples that mentioned before was nearly around 59, 80, 70, and 89% respectively. The higher rates of thermal degradation of these samples at elevated temperatures can be correlated to the evolution of CO₂ gas of maleamic acid moiety as well as the depolymerization occurred for both Cs and PVC as the main constituents of the conjugate.

Water uptake of M_{A-C} Cs-PVC/AgNPs

Table 1 showed the results of water uptake for Cs, amino-PVC and M_{A-C} Cs-PVC/AgNPs samples in buffer solutions at different pH values. The determined values of water uptake represent three successive averages of experiments for each sample. The values of water uptake for the investigated samples showed the higher swelling affinity of M_{A-C} Cs-PVC than both amino-PVC and Cs itself, in all investigated pH values. The results

clearly showed that all samples swelled well at pH 4 compared to pH 7 and 9. Regarding Cs, its water uptake properties are due to the protonation of the NH₂ groups present in its backbone chains in the acidic medium, while at high pH values the inherent hydrophobicity of Cs or its derivatives is dominating [33]. When Am-PVC is taken into consideration, it exhibited a relative degree of swelling which may be due to the terminal NH₂ groups that are resulted in its modification with EDA units, since PVC itself is highly hydrophobic in nature. The higher values of water uptake of MCs-PVC can be rationalized on the basis of the structure of the modified polymer. The presence of some Cs units having free NH₂ groups, in addition to the presence of more than amide group in the modified polymeric chains with a probability of hydrogen bond formation enhanced this ability for water uptake. The high water uptake values of the modified polymers can also be attributed to the spaces created by the effect of the introduction of both linker and modifiers which permits water to diffuse between polymeric chains. Introduction of maleamic acid derivatives in the backbone of the modified polymers increased its water uptake affinity due to the presence of polar carbonyl groups that enhancing the hydrophilicity and then swelling properties. The M_A Cs-PCV sample exhibited also much more swelling properties than the other samples and this may be due to the hydrophilicity nature of the nitro-maleamate derivative when compared to both OMe and Me groups. The observed behavior of the modified polymers towards water uptake may be considered of important outcomes in the field of biomedical applications [46].

Antibacterial activity of M_{A-C} Cs-PVC/AgNPs

The antibacterial activity of the prepared samples, M_{A-C} Cs-PVC/AgNPs, with their different derivatives was investigated against four pathogenic bacterial strains. These strains were classified as Gram-positive (*B. Subtilis*, *S. aureus*) and Gram-negative (*E. coli*, and *P. aeruginosa*) bacteria. Antibacterial activity of Cs, PVC and amino-PVC was also investigated for comparison and ampicillin was used as a standard antibacterial agent. Results of the antibacterial behavior of all investigated samples that are represented by the given inhibition zones are shown in Table 2. It is observed that the three modified polymers with different maleamate derivatives are characterized by higher antibacterial efficiency against the four bacterial strains, in particular the Gram-

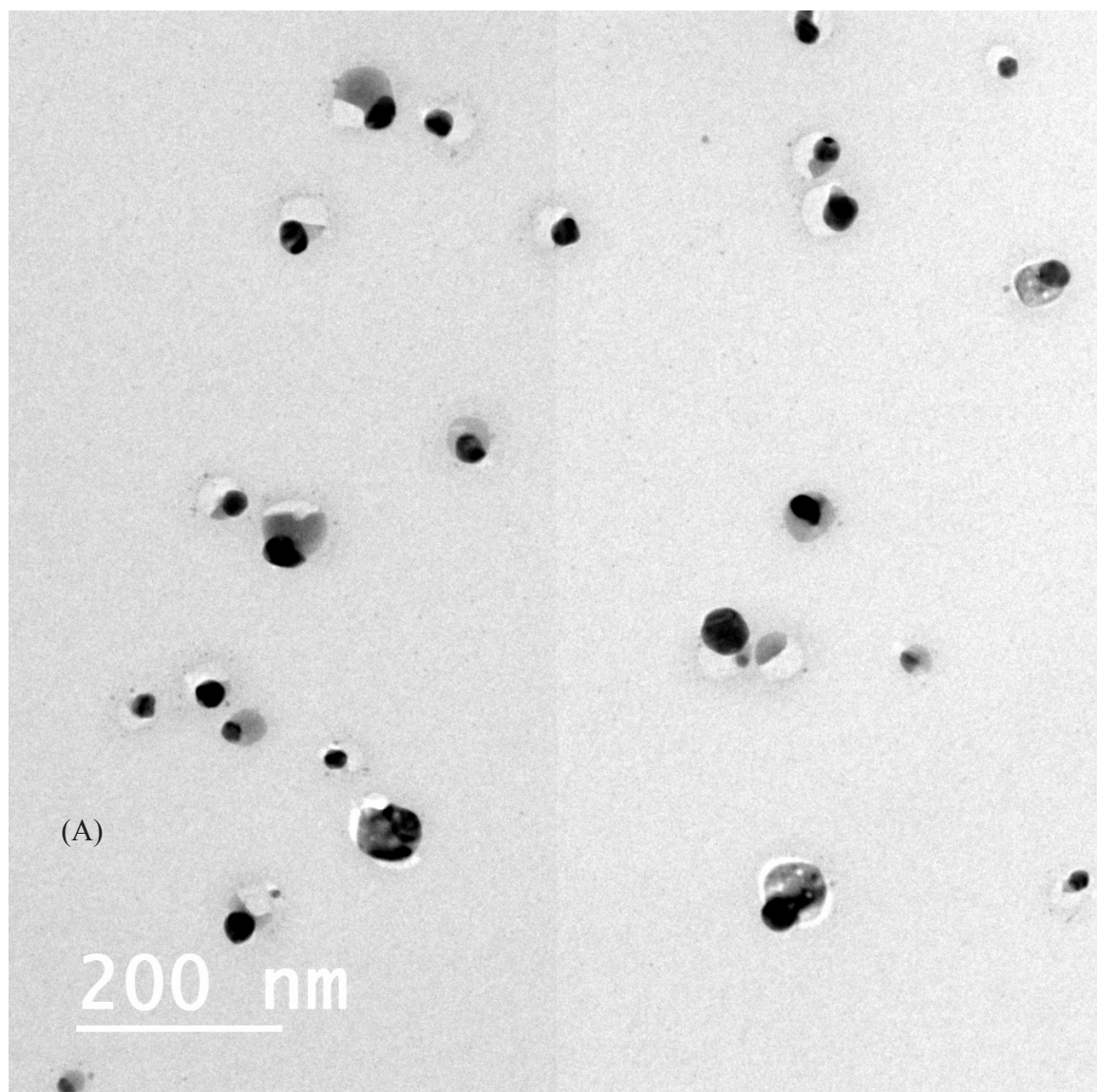


Figure 3(A).

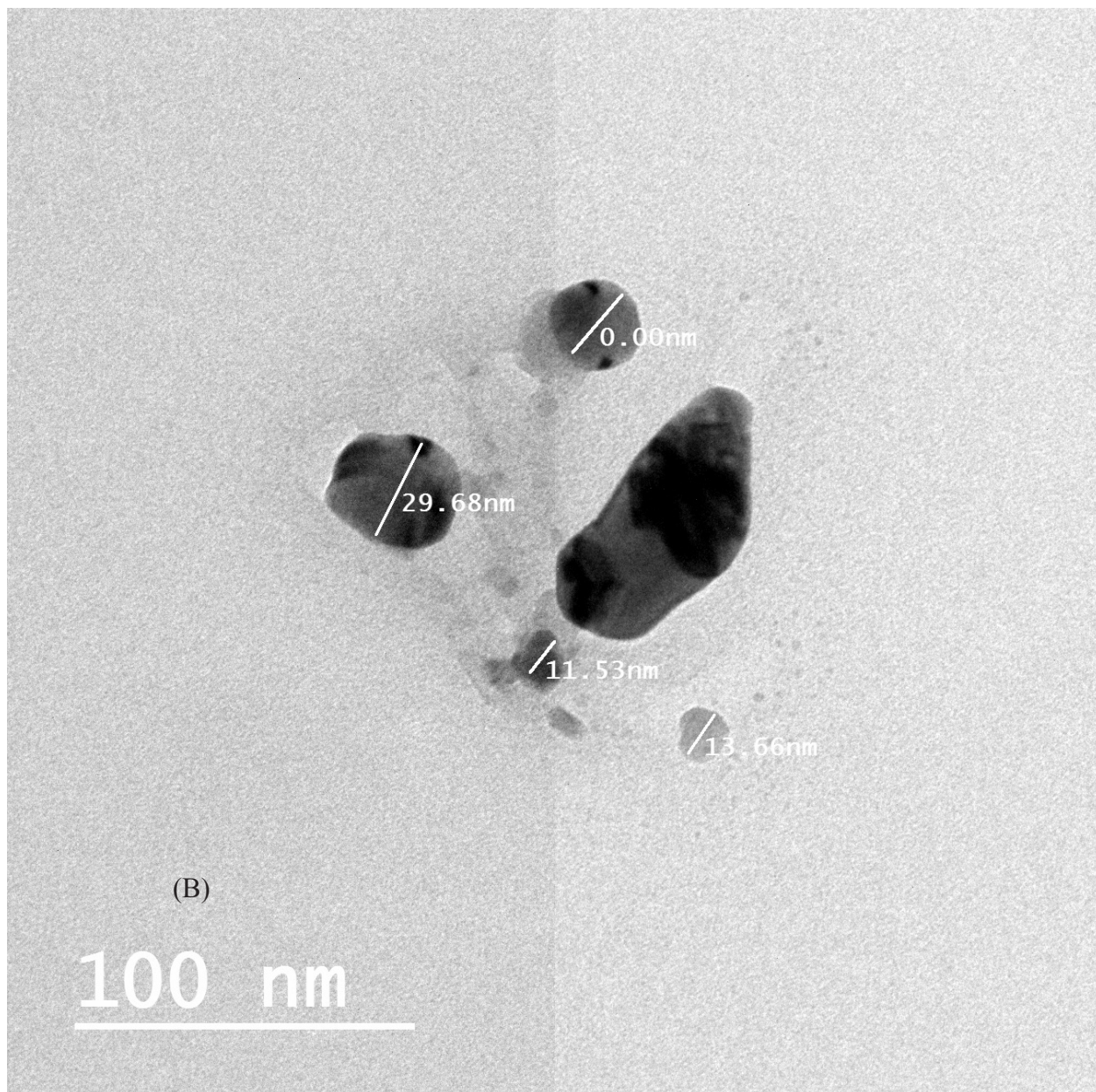


Figure 3(B).

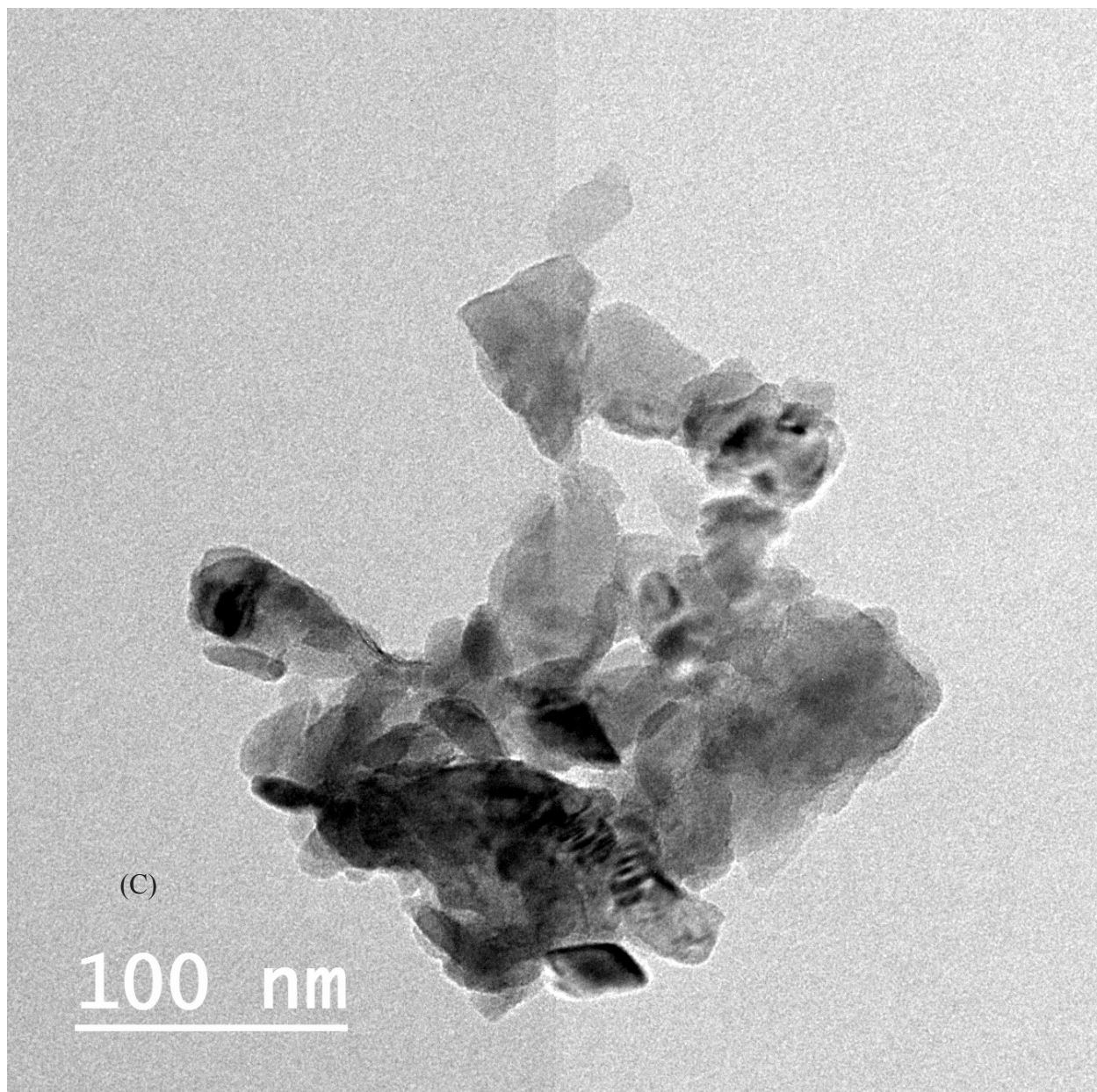


Figure 3(C).

Figure 3. TEM micrographs for M_A Cs-PVC/AgNPs, M_B Cs-PVC/AgNPs, and M_C Cs-PVC/AgNPs.

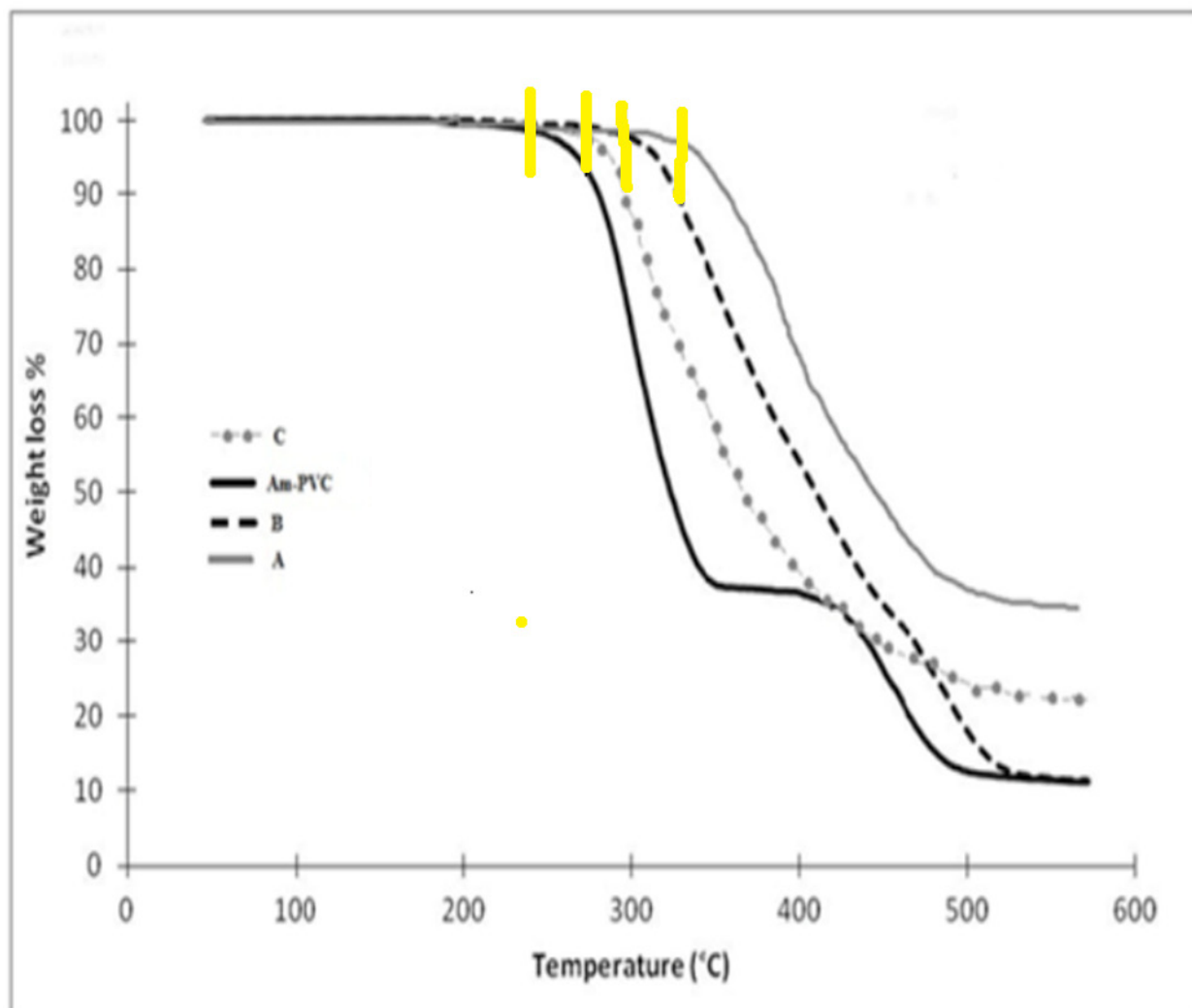


Figure 4. Thermograms of (A), M_A Cs-PVC/AgNPs, (B), M_B Cs-PVC/AgNPs, (C) M_C Cs-PVC/AgNPs, and amino-PVC.

positive ones, when compared to either Cs or amino-PVC samples. Values of antibacterial activity of Cs and Am-PVC are higher than that of nonmodified PVC which is characterized by its poor antibacterial activity and this may be due to the effect of their free amino groups which can be easily protonated to form such compounds having $(\text{NH}_3)^+$ with positively charged nature. This type of compounds with cationic nature has high potency to attack the bacterial cell membrane that may disrupt all the vital process of the microbe leading to either inhibition of bacterial growth or even death of the microbe [47]. It is observed that in case of investigation of antibacterial activity of the modified polymers against the two Gram-positive bacterial strains (*B. Subtilis* and *S. aureus*), the inhibition zones of the $\text{M}_A\text{Cs/PVC/AgNPs}$ with the modifier *p*-nitrophenyl maleamate derivative are 18 and 16 mm with antibacterial activity reached 90 and 88.8% respectively, when compared to the standard antibacterial drug. The same modified polymer exhibited lower antibacterial efficiency against the two examined Gram-negative bacteria (*E. coli* and *P. aeruginosa*) which were found to be 68.2 and 70% with respect to the reference antibacterial agent. For the polymer modified with M_B , its antibacterial activity against the same two strains (*B. subtilis* and *S. aureus*) were 75 and 72.2%, while this activity reached 59 and 65% against the two tested Gram-negative bacteria (*E. coli* and *P. aeruginosa*). All the above values are in comparison with ampicillin as a standard antibacterial agent. Results of Table 2 indicated also that the modified polymer M_C has lower inhibition potency against the examined bacterial strains. The antibacterial activity of the prepared modified polymers can be discussed on the basis of their chemical structures and the effective function groups that may enhance their inhibitory potentials for further bacterial growth. The presence of Cs units with their free NH_2 groups is considered to have a direct effect on the antibacterial potency of the samples. Introduction of the acetyl moiety as a linker between the polymeric chains of amino-PVC and Cs units increased the hydrophilicity of the two polymers as well. This may play an important role in increment of the solubility of the prepared modified polymers to enlarge their antibacterial activity. It is clearly noticed also that the maleamate nitro derivative, between the other ones, exhibited the higher antibacterial potency when compared with ampicillin as a reference antibacterial drug.

This may be due to the withdrawing effect of the nitro group that can increase the cationic nature of the modified polymer. This increase in cationic properties of the samples increases its ability to attack the cell wall membrane of the microbes via the electrostatic interaction between the positively charged compound and the anionic components of the bacterial cell surface [48-49].

The last factor affecting the antibacterial activity of the modified polymers is the incorporation of AgNPs into the polymeric matrix. SEM and TEM micrographs showed that AgNPs have been synthesized and well deposited through the polymeric matrix, in addition to its formation in a uniform distribution as elemental silver. The important role of AgNPs present in these modified polymers is their ability to binding with the DNA of the bacterial cell causing inhibition of bacterial replication with deactivating their vital functions [50]. All the above-obtained results for the prepared modified polymers are promising and recommended to be used in various biomedical applications.

Conclusions

PVC was aminated by its reaction with EDA to give amino-PVC that has been modified by introduction of Cs through chloroacetyl chloride as a linking agent and some maleamic acid derivatives as modifiers, in presence of AgNO_3 (3% w/w) to enhance the antibacterial properties of PVC to be used in various biomedical applications. The maleamic acid derivatives used in this modifications were (*p*-nitrophenyl, *p*-anisyl, and *p*-toluyl) to produce $\text{M}_{A-C}\text{Cs-PVC/AgNPs}$ derivatives. The FTIR spectral data confirmed the chemical structures of the modified polymers. Morphological investigations were performed by carrying out SEM and TEM electron microscopy. The SEM micrographs of the synthesized $\text{M}_{A-C}\text{Cs-PVC/AgNPs}$ nanocomposite showed the surface homogeneity of the polymer and AgNPs are well adhered and uniformly distributed on the polymeric surface. EDX spectrum showed that the Ag contents in the modified polymers, $\text{M}_{A-C}\text{Cs-PVC/AgNPs}$, were 3.17, 1, and 1.02%, respectively. The TEM images showed that AgNPs are well uniformly distributed with diameters of 3-29 nm. Thermal gravimetric analysis was also studied to determine the thermal stability of the prepared $\text{M}_{A-C}\text{Cs-PVC/AgNPs}$. Water uptake determination showed that the prepared polymers have high swelling properties

when compared to both Cs and amino-PVC. The antibacterial efficiency of the formed modified polymers was investigated against two Gram-positive (*B. Subtilis* and *S. aureus*), and two Gram-negative (*E. coli* and *P. aeruginosa*) bacteria. This investigation showed that these modified polymers are of good antibacterial activity when compared to Cs, amino-PVC, as well as ampicillin reference antibacterial drug.

Acknowledgment

The authors acknowledge the National Research Centre (NRC) Egypt for funding this

work; Grant number (11090111).

Conflict of Interest

The authors declare no conflict of interest.

TABLE 1. Water uptake of M_{A-C} Cs-PVC/AgNPs in comparison with Cs and amino-PVC.

Sample codes	pH value		
	4	7	9
Cs	245	84	66
amino-PVC	108	53	39
M_A Cs-PVC/AgNPs	357	145	112
M_B Cs-PVC/AgNPs	295	128	96
M_C Cs-PVC/AgNPs	254	96	75

TABLE 2. Agar disk diffusion test (ADDT) for the antimicrobial activity of tested nanocomposites against bacterial strains.

Sample	Inhibition zone diameter (mm/mg sample)			
	<i>B. subtilis</i>	<i>S. aureus</i>	<i>E. coli</i>	<i>P. aeruginosa</i>
	Gram-positive		Gram-negative	
Cs	11	10	9	9
PVC	7	5	6	5
Amino-PVC	10	11	8	9
M_A Cs-PVC/AgNPs	18	16	15	14
M_B Cs-PVC/AgNPs	15	13	13	13
M_C Cs-PVC/AgNPs	14	14	12	10
DMSO	0.0	0.0	0.0	0.0
Ampicillin	20	18	22	20

References

1. Kenawy, E.; Worley, S. D.; Roy B., The chemistry and applications of antimicrobial polymers: A State of the Art Review. *Biomacromolecule*. 8, 1359–1384 (2007).
2. Frost, M. C.; Reynolds, M. M.; Meyerhoff, M. E., Polymers incorporating nitric oxide releasing/generating substances for improved biocompatibility of blood-contacting medical devices. *Biomaterials*. 26, 1685–1693 (2005).
3. Jones, D. S.; Djokic, J.; Gorman, S. P., The resistance of polyvinylpyrrolidone iodine-poly(-caprolactone) blends to adherence of *Escherichia coli*. *Biomaterials*. 26, 2013–2020 (2005).
4. Kennedy, J. F.; Thorley, M., Polymers for the medical industry: Conference Proceedings: Rapra Technology Ltd., Shawbury. *Carbohydrate Polymers*. 44, 175-178 (2001).
5. Bower, C. K.; Parker, J. E.; Higgins, A. Z.; Oest, M. E.; Wilson, J. T.; Valentine, B. A.; Bothwell, M. K.; McGuire, J., Protein antimicrobial barriers to bacterial adhesion: in vitro and in vivo evaluation of nisin-treated implantable materials. *Colloids Surf B-Biointerfaces*. 25, 81–90 (2002).
6. Chen, K. S.; Ku, Y. A.; Lee, C. H.; Lin, H. R.; Lin, F. H.; Chen, T. M., Immobilization of chitosan gel with cross-linking reagent on PNIPAAm gel/ PP nonwoven composites surface. *Mater SciEng C*. 26, 1–7 (2005).
7. Anderson, J.M., Biological responses to materials. *Annu. Rev. Mater. Res.* 3, 81–110 (2001)
8. Chen, X.; Li, C.; Zhang, L.; Xu, S.; Zhou, Q.; Zhu, Y.; Qu, X., Main factors in preparation of antibacterial particles/PVC composite. *China Particuology*. 2, 225-229 (2004).
9. Lakshmi, S.; Pradeep Kumar, S. S.; Jayakrishnan, A., Bacterial adhesion onto azidated poly(vinyl chloride) surfaces. *Journal of Biomed. Mater. Res.* 61, 26-32 (2002).
10. Balazs, D. J.; Triandafillu, K.; Chevolut, Y., Surface modification of PVC endotracheal tubes by oxygen glow discharge to reduce bacterial adhesion. *Surf. Interface. Anal.* 35, 301-309 (2003).
11. Tariq, R.; Sobahi, M. S.; Makki, I.; Magdy, Y. A., Carrier-mediated blends of Chitosan with polyvinyl chloride for different applications. *Journal of Saudi Chemical Society*. 17, 245–250 (2013).
12. Gajbhiye, R.L.; Mahato, S.K.; Achari, A.; Jaisankar, P.; Ravichandiran, V; Immunogenic Potential of Natural Products. In: Sharma A. (eds) *Bioactive Natural Products for the Management of Cancer: from Bench to Bedside*. Springer, Singapore, p.129 (2019).
13. Ravi, K.; Muzzarelli, M. N. V.; Muzzarelli, R. A. A.; Muzzarelli, C.; Sashiwa, H.; Domb, A. G., Chitosan Chemistry and Pharmaceutical Perspectives. *Chemical Reviews*. 104, 6017–6084 (2004).
14. Ravi kumar, M. N. V., Characterization and Biodegradation Studies for Interpenetrating Polymeric Network (IPN) of Chitosan-Amino Acid Beads. *Reactive and Functional Polymers*, 46, 1–27 (2000).
15. Rinaudo, M., Chitin and chitosan: Properties and applications. *Prog. Polym. Sci.*, 31, 603–632 (2006).
16. Zhu, X.; Yang, R.; Gao, W.; Li, M., Sulfur-modified chitosan hydrogel as an adsorbent for removal of Hg(II) from effluents. *Fibers Polym.* 18, 1229-1234(2017).
17. Lu, B.; Lu, F.; Zou, Y.; Liu, J.; Rong, B.; Li, Z.; Dai, F.; Wu, D.; Lan, G., In situ reduction of silver nanoparticles by chitosan-l-glutamic acid/hyaluronic acid: Enhancing antimicrobial and wound-healing activity. *Carbohydr. Polym.*, 173, 556-565 (2017).
18. Liang Ge, L.; You, X.; Huang, K.; Kang, Y.; Chen, Y.; Zhu, Y.; Ren, Y.; Zhang, Y.; Wu, J.; Qian, H., Screening of novel RGD peptides to modify nanoparticles for targeted cancer therapy. *Biomater. Sci.*, 6, 125-135 (2018).
19. Qu, J.; Zhao, X.; Ma, P.X.; Guo, B., pH-responsive self-healing injectable hydrogel based on N-carboxyethyl chitosan for hepatocellular carcinoma therapy., *Acta Biomater.*, 58, 168-180 (2017).
20. Zhao, X.; Kato, K.; Fukumoto, Y.; Nakamae, K., Synthesis of bioadhesive hydrogels from chitin derivatives. *Int. J. Adhes.*, 21, 227-232 (2001).

21. Lam, B.; Deon, S.; Morin-Crini, N.; Crini, G.; Fievet, P., Polymer-enhanced ultrafiltration for heavy metal removal: Influence of chitosan and carboxymethyl cellulose on filtration performances., *J. Clean. Prod.*, 171, 927-933 (2018).
22. Rai, M. K.; Deshmukh, S. D.; Ingle, A. P.; Gade, A. K., Silver nanoparticles: The powerful nanoweapon against multidrug-resistant bacteria. *J. Appl. Microbiol.*, 112, 841-852 (2012).
23. Franci, G.; Falanga, A.; Galdiero, S.; Palomba, L.; Rai, M.; Morelli, G.; Galdiero, M., Silver nanoparticles as potential antibacterial agents. *Molecules*, 18, 8856-8874 (2015).
24. Donlan, R. M.; Costerton, J. W., Biofilms: Survival mechanisms of clinically relevant microorganisms. *Clin. Microbiol. Rev.*, 15, 167-193 (2002).
25. Taraszkiewicz, A.; Fila, G.; Grinholc, M.; Nakonieczna, J., Innovative strategies to overcome biofilm resistance. *Biomed. Res. Int.*, 2013, 150653 (2013).
26. Biel, M. A.; Sievert, C.; Usacheva, M.; Teichert, M.; Balcom, J. Antimicrobial photodynamic therapy treatment of chronic recurrent sinusitis biofilms. *Int. Forum Allergy Rhinol.*, 1, 329-334 (2011).
27. Machovsky, M.; Kuritka, I.; Bazant, P.; Vesela, D.; Saha, P., Antibacterial performance of ZnO-based fillers with mesoscale structured morphology in model medical PVC composites. *Mater Sci Eng C*, 41, 70-77 (2014).
28. Gaballah, S. T.; El-Nazer, H. A.; Abdel-Monem, R. A.; El-Liethy, M. A.; Hemdan, B. A.; Rabie, S. T., Synthesis of chitosan-PVC conjugates encompassing Ag nanoparticles as antibacterial polymers for biomedical applications. *Int. J. Biol. Macromol.*, 121, 707-717 (2019).
29. Gaballah, S. T.; Khalil, A. M.; Rabie, S. T., Thiazole Derivatives-Functionalized Polyvinyl Chloride Nanocomposites with Photostability and Antimicrobial Properties *J. Vinyl Addit. Technol.*, 25, E137 -E146 (2019).
30. Searle, N. E., Synthesis of nu-aryl-maleimides (E I du Pont de Nemours and Co). US2444536A, (1948).
31. Sauers, C. K., The dehydration of N-arylmaleamic acids with acetic anhydride *J. Org. Chem.*, 34, 2275 (1969).
32. Conley, N. R.; Hung, R. J.; Willson, C. G., A New Synthetic Route to Authentic N-Substituted Aminomaleimides. *J. Org. Chem.*, 70, 4553-4555 (2005).
33. Kang-Chien, L.; Ching-Yun, S., Synthesis of N-(Homocyclylcarbamoyl)-Maleamic Acids and - Maleimides. *J. of Chinese Chem. Soc.*, 25, 77-82 (1978).
34. Mohy Eldin, M. S.; Tamer, T. M.; Abu Saied, M. A.; Soliman, E. A.; Madi, N. K.; Ragab, I.; Fadel, I., Click Grafting of Chitosan onto PVC Surfaces for Biomedical Applications *Adv. Polym. Technol.*, 37, 21640-21651 (2018).
35. Martinez-Quirozad, M.; Lopez-Maldonado, E. A.; Ochoa-Teran, A.; Pina-Luis, G. E.; Oropeza-Guzman, M. T., Modification of chitosan with carbamoyl benzoic acids for testing its coagulant-flocculant and binding capacities in removal of metallic ions typically contained in plating wastewater. *Chem. Eng J.*, 332, 749-756 (2018).
36. Jeong, J. H.; Shin, K. S.; Lee, J. W.; Park, E. J.; Son, S., Analysis of a novel class 1 integron containing metallo- β -lactamase gene VIM-2 in *Pseudomonas aeruginosa*. *J. Microbiol.*, 47, 753-759 (2009).
37. Kanokwiroon, K.; Teanpaisan, R.; Wititsuwannakul, D.; Hooper, A. B.; Wititsuwannakul, R., Antimicrobial activity of a protein purified from the latex of *Hevea brasiliensis* on oral microorganisms. *Mycoses*, 51, 301-307 (2008).
38. In National Committee for Clinical Laboratory Standards, Reference method for Broth Dilution Antifungal susceptibility testing of Conidium-Forming Filamentous Fungi: proposed guideline M38-A. NCCLS, Wayne, PA, USA. (2002).
39. Liebowitz, L. D.; Ashbee, H. R.; Evans, E. G. V.; Chong, Y.; Mallatova, N.; Zaidi, M.; Gibbs, D., A two year global evaluation of the susceptibility of *Candida* species

- to fluconazole by disk diffusion. *Diagn. Microbiol. Infect. Dis.*, 4, 27–33 (2001).
40. Matar, M. J.; Ostrosky-Zeichner, L.; Paetznick, V. L.; Rodriguez, J. R.; Chen, E.; Rex, J. H., Correlation between E-test, disk diffusion, and microdilution methods for antifungal susceptibility testing of fluconazole and voriconazole. *Antimicrob. Agents Chemother.*, 47, 1647-1651 (2003).
41. Zentz, F.; Valla, A.; Le Guillou, R.; Labia, R.; Mathot, A. G.; Sirot, D., Synthesis and antimicrobial activities of *N*-substituted imides. *Farmaco*, 57, 421–426 (2002).
42. Sortino, M.; CechinelFilho, V.; Correa, R.; Zacchino, S., *N*-Phenyl and *N*-phenylalkyl-maleimides acting against *Candida* spp.: Timeto- kill, stability, interaction with maleamic acids. *Bioorg Med Chem.*, 16, 560–568 (2008).
43. AMMARI, F.; MEGANEM, F., Poly(vinyl chloride) functionalization by aliphatic and aromatic amines: application to the extraction of some metal cations. *Turk J Chem.*, 38, 638 – 649 (2014).
44. Queiroz, M.F.; Melo, K.R.T.; Sabry, D.A.; Sasaki, G.L.; Rocha, H.A.O, Does the Use of Chitosan Contribute to Oxalate Kidney Stone Formation?. *Mar. Drugs.*,13, 141-158 (2015).
45. Vimala, K.; Mohana, Y. M.; Sivudu, K. S.; Varaprasad, K.; Ravindra, S.; Reddy, N. N.; Padma, Y.; Sreedhar, B.; Mohana Raju, K., Fabrication of porous chitosan films impregnated with silver nanoparticles: A facile approach for superior antibacterial application. *Colloids Surf B*, 76, 248-258 (2010).
46. Malafaya, P. B.; Pedro, A. J.; Peterbauer, A.; Gabriel, C.; Redl, H.; Reis, R. L., Chitosan particles agglomerated scaffolds for cartilage and osteochondral tissue engineering approaches with adipose tissue derived stem cells. *J. Mater. Sci.: Mater. Med.*, 16, 1077–1085 (2005).
47. Elkholy, S. S.; Khalil, K. D.; Elsabee, M. Z., Homogeneous and heterogeneous grafting of 4-vinylpyridine onto chitosan. *J Appl. Polym. Sci.*, 99, 3308-3317 (2006).
48. Cai, J.; Dang, Q.; Liu, C.; et al., “Preparation, characterization and antibacterial activity of O-acetyl-chitosan-N-2-hydroxypropyl trimethyl ammonium chloride,” *International Journal of Biological Macromolecules*, 80, 8–15 (2015).
49. Feng, QL.; Wu, J.; Chen, G. Q.; Cui, F. Z.; Kim, T. N.; Kim, J. O., A mechanistic study of the antibacterial effect of silver ions on *Escherichia coli* and *Staphylococcus aureus*. *J Biomed Mater Res.*, 52, 662-668 (2000).
50. Mijndonckx, K.; Leys, N.; Mahillon, J.; Silver, S.; Van Houdt, R., Antimicrobial silver: uses, toxicity and potential for resistance. *Bio Metals*. 26, 609-621 (2013).